Chapter 6
Transmitter Design for MIMO Wireless Communications

The high demand for broadband multimedia Internet access and wireless connections has increased the need for more advanced and sophisticated wireless communication systems. However, wireless channels usually provide limited bandwidth and lower quality links.

The next generation of wireless technologies is targeting two essential goals in their design and development. One is the provision of high-speed data rates up to 100 megabits per second (Mb/s) for mobile users and 1 gigabit per second (Gb/s) for stationary users. Achieving the goal of improving the data rate and increasing the system capacity is feasible through the use of more advanced signal processing and coding techniques, such as spectral efficient 64-QAM (quadrature amplitude modulation), orthogonal frequency-division multiplexing (OFDM), and multiple input multiple output (MIMO) topology.

6.1 Complexity and Cost in MIMO Systems

MIMO wireless communication systems are designed to deliver either maximal diversity to enhance transmission reliability or to increase maximal multiplexing gain to support high data rate [1]. The channel capacity and spectral efficiency of a MIMO system is usually much higher than that of a single-input single-output (SISO) system. This can be achieved by employing multiple antennas at the transmitter and receiver.

This performance of a MIMO system can be quantified by the spatial multiplexing gain. Therefore, it is possible to send parallel independent data streams to achieve overall system capacities scaled with $\min(N_t, N_r)$, where N_t and N_r are the number of receiving and transmitting antennas [2]. On the other hand, if the signal copies are transmitted from or received at multiple antennas, this multiantenna system can provide a gain that enhances the reliability of a wireless link. This gain is known as diversity gain, which is achieved by space-time coding. Both diversity and multiplexing gain can be supported by MIMO systems at the same time, but there is a fundamental trade-off between them [1].

In multi-branch transceivers, multiple radio frequency (RF) front-ends are integrated on the same platform. Multiple modulated signals are simultaneously

A. Mohammadi et al.: RF Transceiver Design for MIMO Wireless Communications, LNEE 145, pp. 129–149.
springerlink.com

transmitted and received using these RF front-ends. The multi-branch MIMO transceiver is a simple case of MIMO transceiver architecture, which can improve the power and diversity gains of the system. Transmitter and receiver nonlinearity, modulator imbalance and other impairments should be considered in the design of each branch of a multi-branch transceiver. In addition, when multiple transmission/reception paths are realized on the same chipset, new issues are generated, such as RF crosstalk between the multiple paths, which are due to the proximity of the different circuits [3].

A multi-branch transceiver with N antennas at the transmitter and N antennas at the receiver is demonstrated in Figure 6.1. This system uses multiple parallel RF front-ends, and the number of RF front-ends is equal to the number of antennas. At the receiver, the baseband processing unit decodes N received baseband paths to recover the signal and also to obtain the diversity gain.

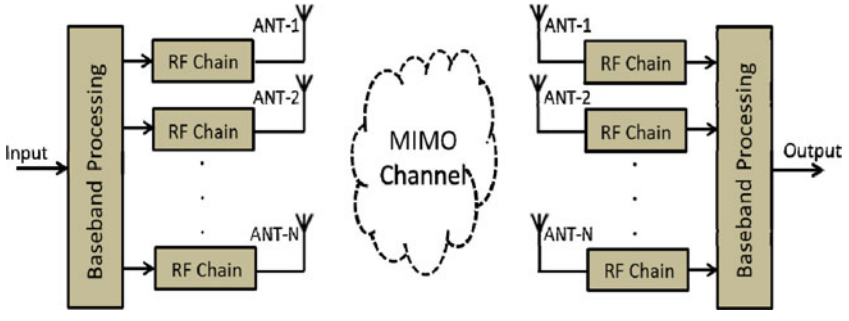

Fig. 6.1 A conventional multiantenna receiver

The multiple antenna RF front-end architecture design usually leads to higher complexity and hardware costs in the RF section. Furthermore, increasing the number of antennas causes growth in RF circuit mismatches and coupling. In fact, these issues limit the application of a high number of antennas at the transceiver. One option to overcome such a problem is the adoption of a single RF front-end in a MIMO system, where a single RF path is implemented instead of multiple parallel RF paths [2], [4]. This reduces the complexity and cost of an RF section and also enables a compact design with lower power consumption.

An orthogonal transmission of multiple RF streams over a single front-end must be identified for the realization of a single RF front-end path. Common designs that may be used for a single receiver front-end realization are the antenna selection technique [5], frequency-division multiplexing, time-division multiplexing [1], and code-division multiplexing [6].

6.2 Transmitters Architectures

Several architectures have been proposed for transmitters in wireless communications, which are dependent on the performance requirements.

6.2.1 Direct Conversion Transmitter

The direct conversion transmitter architecture has received considerable attention for multi-standard, multi-band applications, due to its smaller number of components and usability. This architecture consists of a digital baseband processing unit, digital-to-analog converters (DACs), a direct up-converter, a PA, and an antenna. The digital baseband processing unit has the responsibilities of digital modulation, coding and filtering, in order to develop and synthesize an appropriate transmission signal from the digital input data.

The DACs convert the digital in-phase (I) and quadrature (Q) baseband signals to analog signals, which feed the quadrature modulator for direct up-conversion. Analog signals are directly up-converted to the RF with I and Q carriers. The block diagram of a direct conversion transmitter is shown in Figure 6.2. The bandpass filter after the signal summation is used to suppress the out-of-band signals produced by the harmonic distortion of the carrier. The RF signal power is increased by the PA for transmission through the antenna.

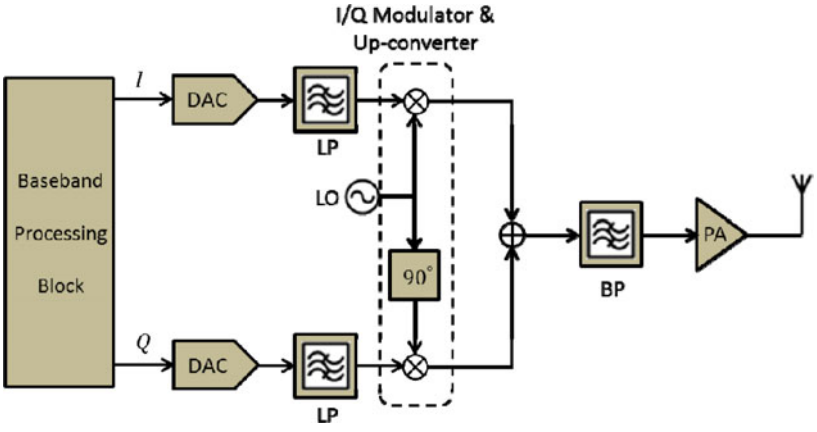

Fig. 6.2 Block diagram of a direct conversion transmitter

The direct conversion transmitter is theoretically simple, and there are no intermediate frequency (IF) components. The drawbacks of this architecture are local oscillator (LO) leakage at RF frequencies, voltage controlled oscillator (VCO) pulling, and the requirement of an I/Q mixer at RF frequencies [7]. The direct conversion transmitter suffers from unequal complex gains of the I and Q paths. This depends on the frequency and operating temperature. The quality of the output RF signal is strongly affected by the I/Q imbalance caused by the modulators.

In addition, the PA stage has nonlinear behavior, which deteriorates the output signal quality and produces out-of-band power emission. Digital predistortion (DPD) techniques are suitable candidates to enhance the signal quality and compensate for the out-of-band power. However, the I/Q imbalance at the transmitter can considerably reduce the linearization capacity of the digital predistorter [8].

6.2.2 *Superheterodyne Transmitter*

The most common double conversion approach is the superheterodyne architecture. A schematic of a superheterodyne transmitter is shown in Figure 6.3. In the first stage, the baseband input is up-converted to IF by an I/Q mixer. The first bandpass filter, BP1, shown in this figure reduces any spurious out-of-band power prior to the second up-conversion. In the second stage, the IF signal goes through a second up-conversion to achieve the desired transmit frequency. A second bandpass filter, BP2, can be utilized to filter additional spurious out-of-band power caused by the second mixing operation [9]. The IF frequency is determined by the first LO frequency, f_1. Two frequencies are generated by the second mixer stage, $f_2 + f_1$ and $f_2 - f_1$. One of the frequencies is selected by the second bandpass filter and the unwanted frequency (image frequency) is rejected.

The superheterodyne architecture was developed to overcome the inherent problems in the direct conversion or homodyne architecture. In this architecture, some of the unwanted frequency components originating from nonlinearities (e.g., in the mixers) can be removed by filters. Figure 6.4 shows the frequency plan of the superheterodyne transmitter with one IF frequency.

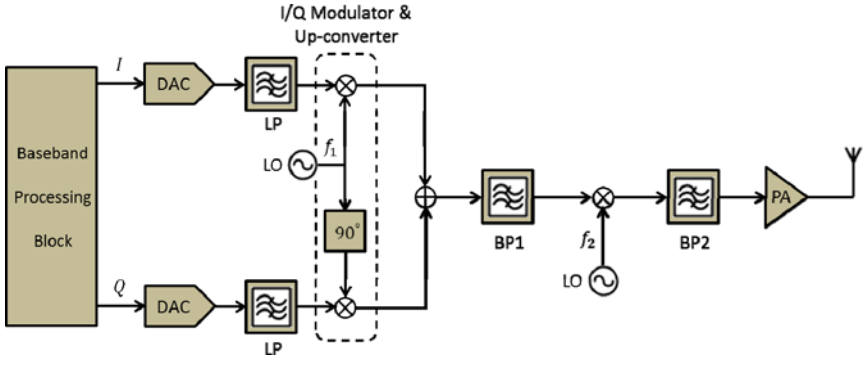

Fig. 6.3 Block diagram of a superheterodyne transmitter

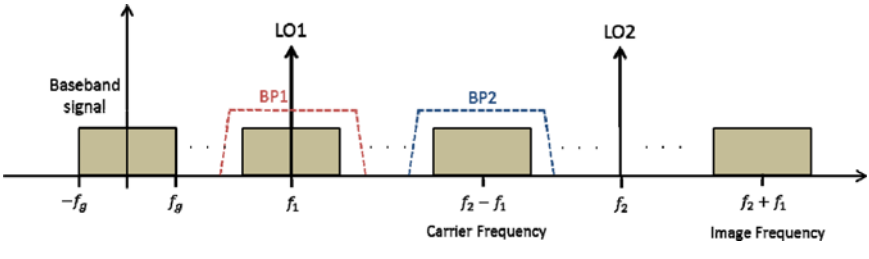

Fig. 6.4 Frequency plan of the superheterodyne transmitter

6.3 Brief Overview of MIMO Transmission Schemes

In telecommunications, multiplexing is a technique by which multiple analog signals or digital data streams are combined into a single signal to be transmitted over a shared medium. The basis of the multiplexing technique is the division of the entire signaling dimensions into parts or channels and the allocation of these parts or channels to different users. The most common techniques of dividing signal space are along the frequency, time and code axes, which are called frequency-division multiplexing (FDM), time-division multiplexing (TDM), and code-division multiplexing (CDM).

6.3.1 FDM Technique

FDM is a technique that combines several signals into one medium by sending signals in several distinct frequency ranges over that medium, as shown in Figure 6.5 (a). This is a familiar technique in many industries, such as telephone and commercial radio and television broadcasting. Although the FDM technique can be applied to both analog and digital systems, it has been widely used in the analog communication systems.

Guard bands are used in the FDM technique to avoid interference between channels. The FDM produces a spectral efficiency, which is due to the transmission rate that is quite close to the maximum rate needed by the user. FDM needs frequencies that can provide different carriers with different channels, because the transmission in communication systems is continuous.

6.3.2 TDM Technique

TDM is a multiplexing technique that allows more than one user to access RF channels without any interference between them. Figure 6.5 (b) shows how the frequency channels are shared at different times. It involves the sequencing of groups of signals from each individual input, so that they can be associated with the appropriate receiver. TDM has been used in digital communication technologies, including significant application in cellular phone technologies. The guard times are used in the TDM technique to reduce the transmission impairments, such as delay propagation, the transient response of the pulse signal, and other impairments.

6.3.3 CDM Technique

CDM is a multiplexing technique where several channels share the same frequency spectrum at the same time, as shown in Figure 6.5 (c). CDM employs spread-spectrum technology and a special coding method in which each transmitter is

assigned a code, allowing multiple users to be multiplexed over a shared physical medium. Direct sequence spread spectrum (DSSS) and frequency hopping are two forms of the CDM technique. In CDM, the modulated coded signal has a much higher bandwidth than the data being communicated. One of the early applications for CDM is in Global Positioning Systems (GPSs). CDM techniques are also used in wireless networks due to the advantage of reducing the interference among different users.

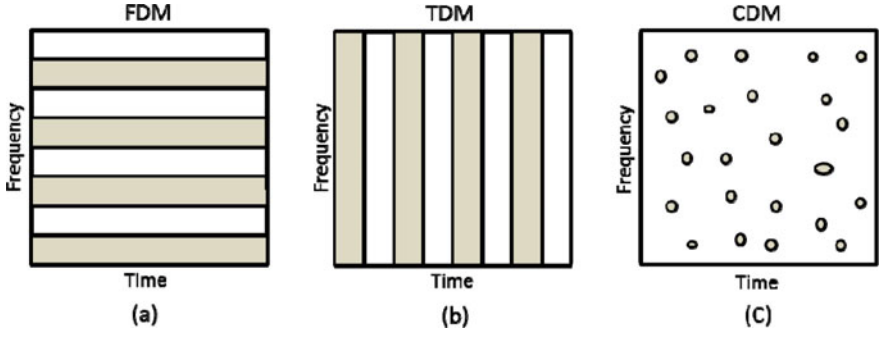

Fig. 6.5 Time and/or frequency sharing in (a) TDM, (b) FDM and (c) CDM techniques

6.4 MIMO Transceiver Architectures

MIMO refers to a system where multiple inputs have interaction with multiple outputs. In the context of wireless communications, MIMO refers to topologies in which multiple modulated signals, separated in the space, time or frequency domain are simultaneously transmitted through an RF front-end. A MIMO system with modulated signals separated in the space domain is are already known as a MIMO system in wireless communication theory. This topology has multiple branches of RF front-ends that are involved in simultaneous transmission of signals. A MIMO system with modulated signals separated in the frequency domain is a system in which multiple signals modulated in different carrier frequencies are transmitted all together through a single-branch RF front-end.

6.4.1 Antenna Selection Architecture

Antenna selection techniques in spatial multiplexing at the transmitter and/or receiver can lead to simpler RF front-end MIMO systems. Based on antenna selection techniques, some of the available antennas are chosen; therefore, fewer RF chains than the number of transmitter and/or receivers antennas are used. Consequently, this reduces cost and complexity; and, at the same time, the system performance is maintained. The antenna selection technique, both in the transmitter

and receiver of a MIMO system, is demonstrated in Figure 6.6. Although the implementation of the antenna selection technique in the receiver is straightforward, the implementation in the transmitter needs a feedback path from the transmitter to the receiver [2].

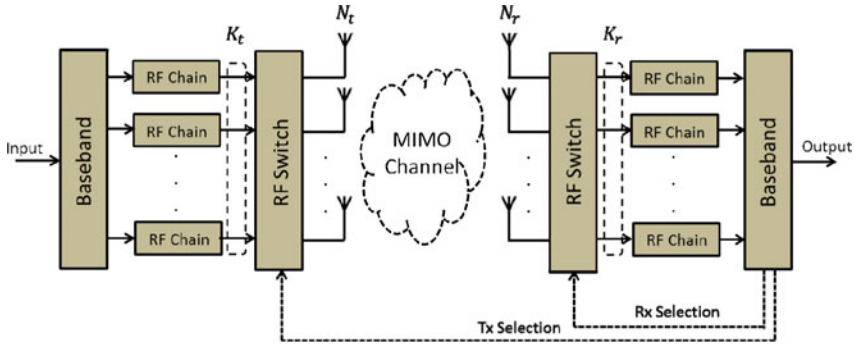

Fig. 6.6 A MIMO system with antenna selection technique

The performance of the antenna selection algorithm is largely dependent on the objective function or the selection criterion utilized to construct the subset of antennas. Several criteria have been introduced. A number of common selection criteria are briefly presented in the following subsections.

6.4.1.1 Maximum Capacity Criterion

Channel capacity maximization is a typical criterion for antenna selection. An analytical bound for the channel capacity of MIMO systems with antenna selection [1], [10] can be given as:

$$C \le \sum_{i=1}^{K_r} \log_2\left(1 + \frac{\rho}{N_t}\gamma_i\right) \tag{6.1}$$

where ρ is the mean signal-to-noise ration (SNR), K_r is the number of selected antennas in the receiver, and γ_i represents the squared norm of the i th row of the MIMO channel matrix, H, which is ordered from the smallest to the largest. Based on the capacity formula in (6.1), the capacities for all possible subsets of a receiver's antennas, $p \in P$, are calculated; and, the subset with the largest capacity C_p is selected.

6.4.1.2 Maximum Minimum Singular Value Criterion

For each subset of receiver antennas, $p \in P$, the minimum singular value ($\lambda_{\min}$) corresponding to different H_p is calculated. Then, the subset with the largest $\lambda_{\min}$ is selected.

6.4.1.3 Norm-Based Selection (NBS) Criterion

In the norm-based selection (NBS) criterion, the subset of receiver antennas related to the rows of H with the largest Euclidean norm is chosen. Although this technique is not optimal when the number of RF front-ends is greater than one [11], it remains a popular criterion because of its simplicity.

6.4.2 Frequency-Division Multiplexing (FDM) Architecture

In FDM architecture, the signals of different antennas are shifted in frequency with mixing by different LOs, added together, and transmitted through a single-branch RF frond-end. Figure 6.7 shows the general block diagram of FDM architecture. The multiple signals from different antennas are separated in the frequency domain. A single RF front-end is used to down-convert the signals, and the frequency shifts of the multiple streams are removed in the baseband block. The diversity gain is extracted by further processing [4]. Examples of this type of system are concurrent dual-band transmitters and multicarrier transmitters.

A system-level performance of a scenario with two antennas at the receiving side was studied in [4]. Considering $s(t)$ as the passband signal with a center frequency, f_c, and a bandwidth, ω, the received signal of the first antenna is $h_1 \cdot s(t) + n_1(t)$; and, the received signal from the second antenna is $h_2 \cdot s(t) + n_2(t)$, where $n_1(t)$ and $n_2(t)$ are the passband noise, and h_1 and h_2 are the Rayleigh flat fading channel coefficients. The signal of second antenna is combined with a low-frequency oscillator at the same frequency (ω), then filtered to remove the IF term.

The deficiency of this technique is the requirement of a narrowband filter in the RF frequency. The simulation results for binary phase shift keying (BPSK) modulation using two antennas are demonstrated in Figure 6.8. The variation between the ideal and simulated curves for diversities 1 and 2 is related to the filter design and its quality factor.

6.4.3 Time-Division Multiplexing (TDM) Architecture

The general block diagram of TDM architecture is shown in Figure 6.9. In this architecture, the same number of antennas as in the conventional topology is used,

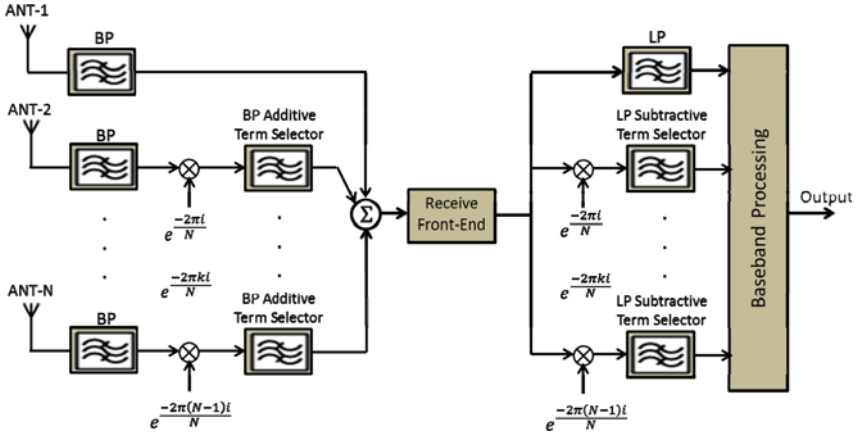

Fig. 6.7 Realization of single-branch multiantenna receiver based on FDM

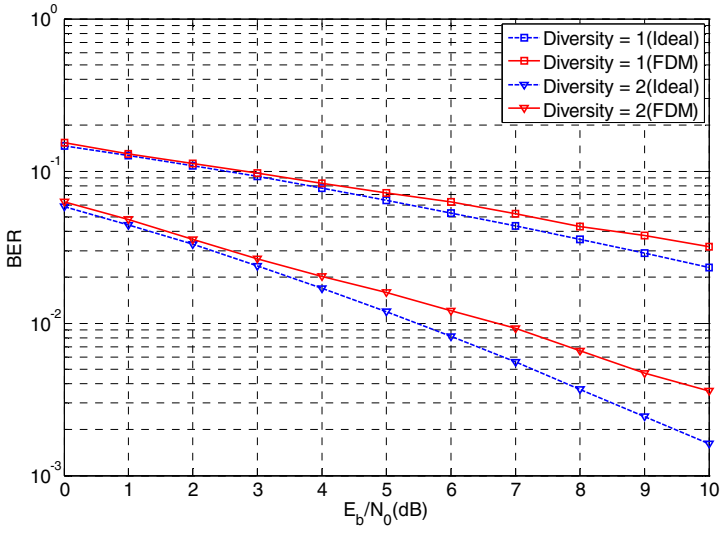

Fig. 6.8 Bit error rate (BER) versus E_b / N_0 for a single frond-end receiver based on FDM using BPSK modulation [4]

but instead of having multiple RF front-ends, a single pole, multiple-throw RF switch along with a single RF front-end are used to down-convert the RF signals to baseband. Furthermore, the signals are carried to the baseband processing unit using a de-multiplexer. The switch is used to capture the signals of all the antennas for every symbol time interval of the modulated signal. This offers some constraints on the switching speed. In addition, careful alignment of the data before

and after the multiplexing and de-multiplexing of the multiple signals in the MIMO receivers is desired.

A single front-end MIMO receiver using the TDM technique can be realized as a single RF architecture by time-multiplexing the antennas' signals using a single-pole multiple-throw RF switch. The received signals are de-multiplexed after RF processing according to a diversity algorithm. Although this architecture implements the same number of antennas as in the conventional architecture, it reduces the number of RF front-ends from N to 1. Consequently, the overall cost and size of the multiantenna receiver and also RF design mismatch are significantly reduced [2].

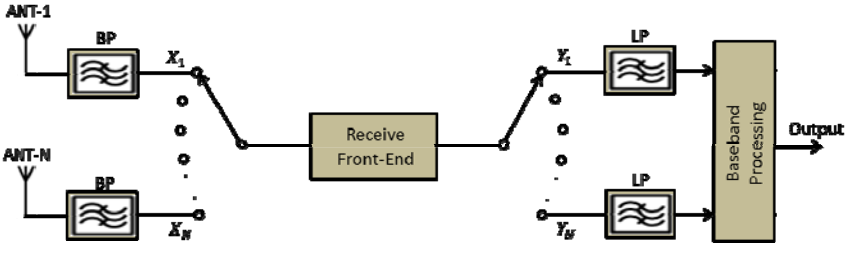

Fig. 6.9 Realization of single-branch multiantenna receiver based on TDM

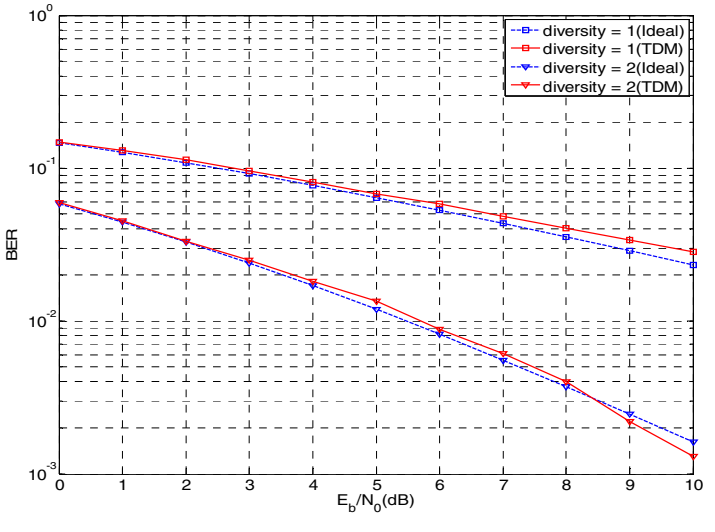

Fig. 6.10 BER versus E_b/N_0 for a single frond-end receiver based on TDM using BPSK modulation [4]

Figure 6.10 shows the results of a time-multiplexed receiver using a raised cosine pulse shape filter with a roll-off factor of 0.5 for single antenna and two-antenna cases using BPSK modulation. Zero forcing (ZF) receivers are implemented. To compare the TDM architecture with a conventional architecture, the bit error rate (BER) of the multiple frond-end systems is demonstrated as well. The diversity gain using a single time-multiplexed RF front-end is equal to the diversity gain of the multiple RF front-end, as shown in Figure 6.10. This architecture demands a wider bandwidth than the one used in the conventional MIMO receiving front-end.

6.4.4 Code-Division Multiplexing (CDM) Architecture

In code-division multiplexing (CDM), the signals from different antennas are multiplied by orthogonal codes and added together. At the receiver, a single RF front-end is used to down-convert the resultant RF signals to baseband, where the signals are again multiplied by the orthogonal codes, integrated, and de-multiplexed. This technique is demonstrated in Figure 6.11. In the case of two receiver antennas, the first and second signals are multiplied by $C_1(t)$ and $C_2(t)$ codes, respectively, in the symbol duration, and then summed together. These codes should be orthogonal, i.e., $C_1(t)$ is equal to 1 between 0 and T_s, and $C_2(t)$ is equal to 1 between 0 and $T_s/2$ and equal to -1 between $T_s/2$ and T_s. T_s is the symbol duration. After summing the signals, the total signal, $(h_1 \cdot s(t) + n_1(t)) \cdot c_1(t) + (h_2 \cdot s(t) + n_2(t)) \cdot c_2(t)$, is down-converted using a single RF front-end. The baseband signal is expressed as $(h_1 \cdot \tilde{s}(t) + \tilde{n}_1(t)) \cdot c_1(t) + (h_2 \cdot \tilde{s}(t) + \tilde{n}_2(t)) \cdot c_2(t)$.

Followed by down-conversion in the baseband processing unit block, the signal is multiplied by $C_1(t)$ and $C_2(t)$. This separates the signal into different paths. An integrator removes the effect of the other signals in each path. However, the effect of the noise of both antennas is preserved in each path. The output of the integrator in the first path can be obtained as:

$$\begin{aligned} & h_1 \cdot \tilde{s} + \tilde{n} = \\ & \frac{1}{T_s} \int_0^{T_s} \left[(h_1 \tilde{s}(t) + \tilde{n}_1(t)) \cdot c_1(t) \cdot c_1(t) + (h_2 \cdot \tilde{s}(t) + \tilde{n}_2(t)) \cdot c_2(t) \cdot c_1(t) \right] dt \\ & = \frac{1}{T_s} \int_0^{T_s} h_1 \tilde{s}(t) dt + \frac{1}{T_s} \int_0^{T_s} \tilde{n}_1(t) dt + 0 + \frac{1}{T_s} \int_0^{T_s} \tilde{n}_2(t) \cdot c_2(t) \cdot c_1(t) dt \end{aligned} \tag{6.2}$$

where $\tilde{s}(t)$ is invariable in the symbol duration, T_s, and the codes have unit energy. The third term is zero, which is due to the orthogonality of $C_1(t)$ and $C_2(t)$; and, $\tilde{s}(t)$ is constant in the symbol duration, T_s. The fourth term is non-zero, because $\tilde{n}_2(t)$ is stochastic and variable in the symbol duration.

The second and fourth terms of the integral have similar power; therefore, the output noise power using CDM is twice that of conventional design. The noise level is increased by $10\log(N)$ dB in each branch, when N antennas are utilized and the signals are down-converted with the CDM technique [12]. Figure 6.12 demonstrates the simulation results for BPSK modulation using two receiving antennas. A separation of 3 dB can be noticed between the CDM technique and the conventional diversity system [4].

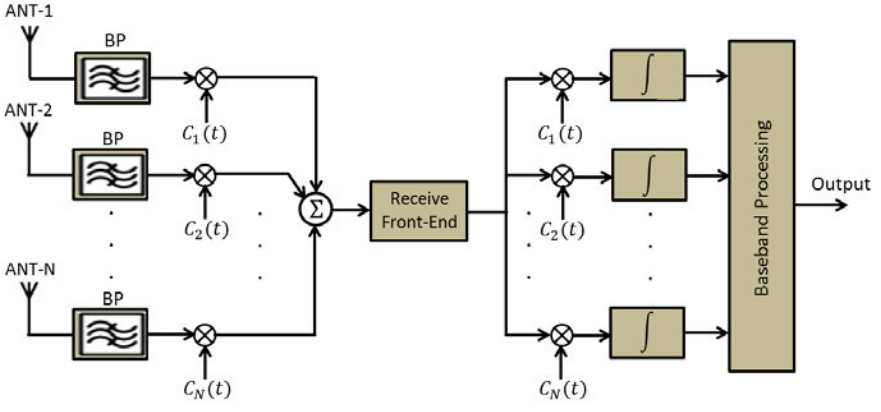

Fig. 6.11 Realization of single-branch multiantenna receiver based on CDM

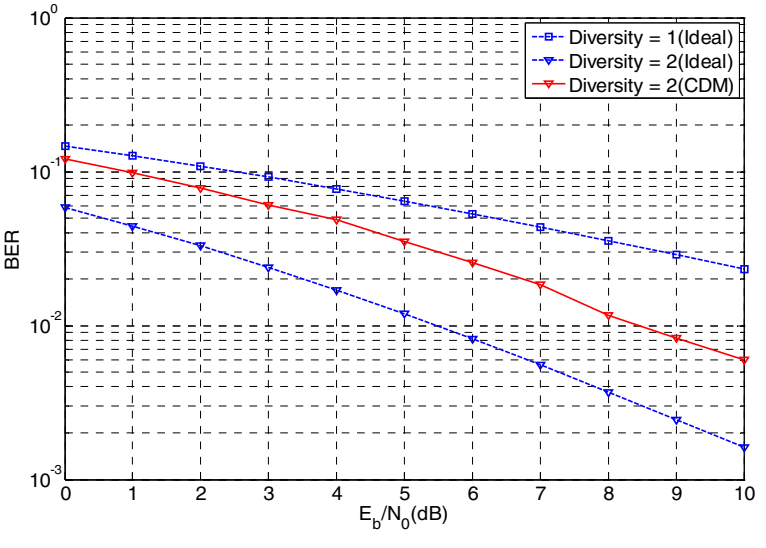

Fig. 6.12 BER versus E_b/N_0 for a single frond-end receiver based on CDM using BPSK modulation [4]

6.5 Distortion and Impairment Compensation in MIMO Transmitters

MIMO topology is a highly efficient solution for improving the spectral efficiency of wireless systems. Indeed, moving from SISO transceivers to MIMO transceivers could theoretically multiply the system capacity or data rate by the number of outputs integrated in the MIMO transceiver. However, MIMO topology faces various implementations issues that can be classified into two major categories. The first category consists of issues related to the general transceiver design, such as transmitter linearity, receiver dynamic range, and imbalance and leakage in mixers [3]. This group is not unique to MIMO systems.

The second category is specific to MIMO transceivers. In multi-branch MIMO transceivers, crosstalk results from the coupling and interference between the signals of different branches. Crosstalk is more likely to take place between the branches, because the signals in different branches use the same operating frequency and have equal transmission power [13]. This is more significant in an integrated circuit (IC) design, especially when the actual footprint of the circuit is small [14].

RF crosstalk can be categorized as linear and nonlinear. Linear crosstalk occurs beyond the output of the transmitter, i.e., at the antenna, and can be modeled as a linear function of the interference and desired signals. This means the signal affected by linear crosstalk does not pass through nonlinear components. Conversely, nonlinear crosstalk affects the signal before it passes through nonlinear components. This crosstalk that takes place in the transmitter circuit prior the PA is the main source of nonlinear crosstalk, since the PA is the main source of nonlinearity [3]. The origin and nature of both types of crosstalk are illustrated in Figure 6.13.

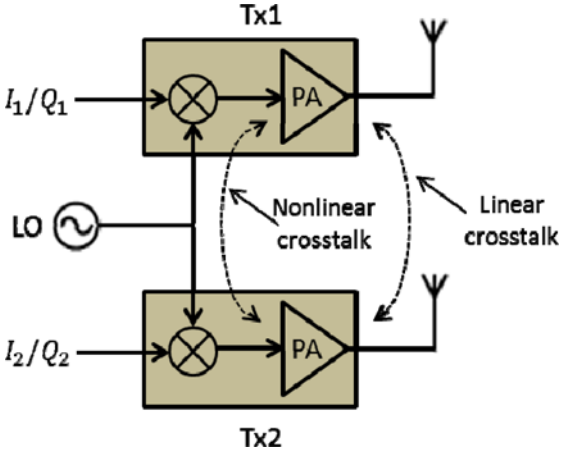

Fig. 6.13 Linear and nonlinear crosstalk in dual-branch MIMO transmitters

6.5.1 Antenna Crosstalk

Antenna crosstalk is the effect of the transmitted signal from one antenna element to another antenna element, which can be modeled as:

$$\vec{Y} = \mathrm{A}\vec{X} \tag{6.3}$$

where $\vec{X} = [x_1 \quad x_2]^T$ and $\vec{Y} = [y_1 \quad y_2]^T$ are the signals at the input and output of the antennas, respectively; and, $\mathrm{A} = \begin{bmatrix} 1 & \alpha \\ \beta & 1 \end{bmatrix}$ is the antenna crosstalk matrix. For symmetric antenna crosstalk, α and β are equal [3].

With the expansion of (6.3), the signals at the output of the antennas after crosstalk can be shown as:

$$\begin{cases} y_1 = x_1 + \alpha x_2 \\ y_2 = \beta x_1 + x_2 \end{cases} \tag{6.4}$$

From this equation, it can be observed that y_1 and y_2 are linear functions of the signals at the antennas' input.

Linear crosstalk has been addressed in several research studies [15], [16]; and, several techniques have been proposed to compensate for it. The compensation is simultaneously performed mostly at the receiver side for the composite linear crosstalk generated at the transmitter and receiver antennas and also by the channel.

A 2×2 MIMO system with three types of linear crosstalk is shown in Figure 6.14. The total linear crosstalk can be modeled as:

$$\vec{Y} = (\mathrm{BHA})\vec{X} + \mathrm{B}\vec{N} \tag{6.5}$$

where A and B are crosstalk matrices for the transmitting and receiving antennas, respectively; and, $\mathrm{H} = \begin{bmatrix} h_{11} & h_{12} \\ h_{21} & h_{22} \end{bmatrix}$ is a crosstalk matrix for the channel; and, $\vec{N}$ is an additive white Gaussian channel noise (AWGN) vector.

The uncorrelated received signal using the matrix inversion algorithm is given by:

$$\vec{Y}_{uncorr.} = (\mathrm{BHA})^{-1}\vec{Y} \tag{6.6}$$

Substituting (6.5) into (6.6):

$$\vec{Y}_{uncorr.} = \vec{X} + (\mathrm{HA})^{-1}\vec{N} \tag{6.7}$$

where $\vec{Y}_{uncorr.}$ is the uncorrelated component of the received signal without the noise component [3].

From (6.7), it can be observed that the matrix inversion method is practical if the (BHA) matrix is invertible. Furthermore, the crosstalk in the transmitter antenna and MIMO channel may deteriorate the performance of the MIMO system due to the noise enhancement, as the last term in (6.7). The performance of the MIMO system is not sensitive to the receiver antenna crosstalk as long as matrix **B** is invertible.

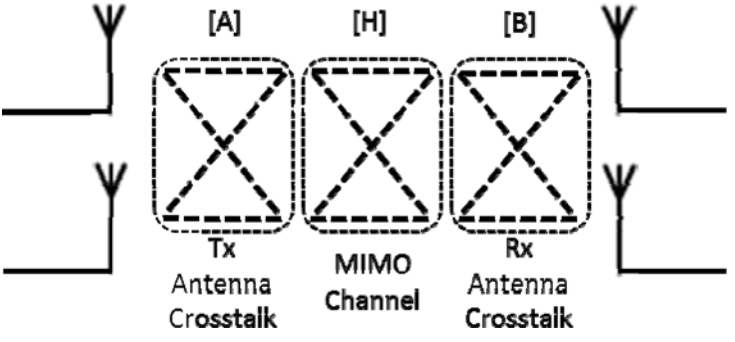

Fig. 6.14 A 2×2 MIMO channel and antenna crosstalk

6.5.2 Nonlinear RF Crosstalk

MIMO transmitters need to maintain certain levels of efficiency and linearity in the system, similar to those of single-branch transmitters. Actually, the power efficiency and linearity requirements of MIMO transmitters are more restrained than those of single-branch transmitters. As demonstrated in Figure 6.13, crosstalk that occurs before the PA is recognized as nonlinear. Some sources of this type of crosstalk can be the leakage of the RF signal through the common LO [14] and interference in the chipset.

Considering RF nonlinear crosstalk and transmitters' nonlinearities, the transmitters' output in a dual-branch MIMO transmitter can be modeled as:

$$y_1 = f_1(x_1 + \alpha x_2) \tag{6.8}$$

$$y_2 = f_2(\beta x_1 + x_2) \tag{6.9}$$

where $f_1(\cdot)$ and $f_2(\cdot)$ are nonlinear functions that represent the transmitter responses of each branch; x_i and y_i are the input and output signals, respectively; and, α and β are the RF nonlinear crosstalk. Since $f_1(\cdot)$ and $f_2(\cdot)$ are nonlinear, a simple matrix inversion is not sufficient to compensate for the effect of nonlinear crosstalk.

Due to unavoidable RF crosstalk between branches of a MIMO transmitter, independent modeling of each branch is not adequate to include the effects of RF nonlinear crosstalk. Hence, the traditional DPD techniques developed for SISO systems are not suitable for MIMO systems. In fact, a new DPD architecture with the capability of having more than one input signal is required [3].

6.5.3 Effects of Nonlinear Crosstalk on DPD Extraction

In Figure 6.15 (a), a MIMO transmitter is shown as a black box with two inputs and two outputs. One way to model the dual-branch MIMO transmitter is independent modeling of each branch of the MIMO transmitter, which is illustrated in Figure 6.15 (b). The independent modeling is reliable if there are no interactions between the two branches. However, as discussed previously, nonlinear crosstalk is an inevitable incident in dual-branch MIMO transmitters. As a matter of the fact, the transmitters' output with the effect of crosstalk can be modeled as in (6.8) and (6.9). It can be observed from the expressions in (6.8) and (6.9) that the signal at the output of each branch is a function of both input signals, in the presence of RF nonlinear crosstalk. Hence, independent modeling of each branch, according to the input and output signals of that branch, leads in an inefficient model for the dual-branch transmitter. Similarly, the use of DPD linearization techniques leads to a similar scenario when linearization blocks are realized separately for each branch of the dual-branch transmitter.

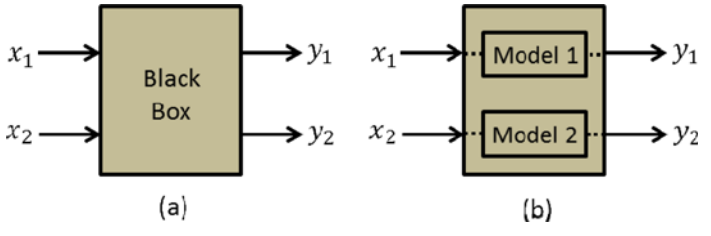

Fig. 6.15 A MIMO transmitter as (a) a black box, (b) two independent parallel models

The cascade of DPD and the RF frond-end complex transfer function in an ideal transmitter without nonlinear crosstalk results in a linear complex transfer function. However, in MIMO transmitters, the quality of the DPD extraction degrades when nonlinear crosstalk modifies the complex envelope of the RF signal at the input of the PA of a transmitter [3]. As shown in Figure 6.16, the DPD coefficients of the upper branch transmitter are extracted using the digital baseband signal to be transmitted (z_1) and the equivalent complex envelope of the PA RF output (y_1). The coupled signal from the second path (z_2) is also added to signal

z_1, and the combined signal ($z_1 + \alpha z_2$) is amplified by the PA. Hence, the output PA signal can be expressed as:

$$y_1 = f_1(z_1 + \alpha z_2) \tag{6.10}$$

In the DPD extraction process, the DPD function, $g_1(\cdot)$, is the inverse function of $f_1(\cdot)$, which depends on both input signals, x_1 and x_2, through z_1 and z_2 terms. Considering that $g_1(\cdot)$ is only a function of the x_1 input signal, the PA output signal is:

$$y_1 = f_1(g_1(x_1) + \alpha z_2) \neq G_0 \cdot x_1 \tag{6.11}$$

where G_0 is the linear or small-signal gain of the PA.

Hence, the nonlinear crosstalk influences the extraction and effectiveness of the DPD function.

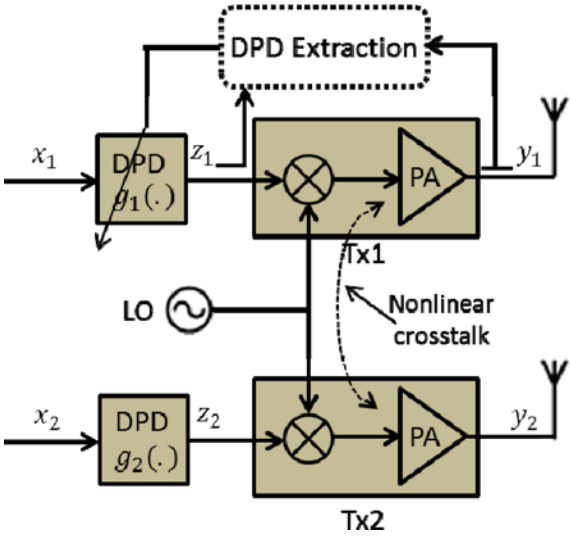

Fig. 6.16 DPD and PA with nonlinear crosstalk in a MIMO system

6.5.4 Impairment and Distortion Compensation

Most of the techniques proposed so far have addressed either nonlinear distortion, the I/Q imbalance of the modulator, or the coupling effects in MIMO transmitters. However, there are not many proposed solutions that jointly address all the issues at the same time. In order to characterize the static and dynamic (memory effect) nonlinear behavior of the transmitter, the multi-branch polynomial model can be

used [17]. The output complex envelope signal at the output of the nonlinear transmitter can be expressed as:

$$y(n) = \sum_{j=0}^{M} \sum_{i=1}^{N} b_{i,j} \cdot x(n-j) \cdot \left| x(n-j) \right|^{i-1} \tag{6.12}$$

where $x(n)$ and $y(n)$ are the input and output complex signal envelopes, respectively; $b_{i,j}$ are the model coefficients of the jth filter tap; and, N and M are the maximum polynomial order and memory depth, respectively.

In a MIMO transmitter, for the modeling of the coupling effects in addition to the PA nonlinearity, each output of the transmitter should contain cross terms between the input signals [3]. The memory polynomial model can be extended for a dual-input dual-output transmitter with crosstalk effects. The signal at each output of the transmitter is given by:

$$\begin{aligned} y_k(n) = & \sum_{j=0}^{M} \sum_{i=1}^{N} b_{k,1,i,j} \cdot x_1(n-j) \cdot \left| x_1(n-j) \right|^{i-1} + \\ & \sum_{j=0}^{M} \sum_{i=1}^{N} b_{k,2,i,j} \cdot x_2(n-j) \cdot \left| x_2(n-j) \right|^{i-1} \end{aligned} \tag{6.13}$$

where $x_1(n)$ and $x_2(n)$ are the input complex signals envelopes, and $y_k(n)$ is the output complex signal envelop at the k -branch of the MIMO transmitter. The modeling of the nonlinear crosstalk (memoryless case) in a MIMO transmitter is illustrated in Figure 6.17.

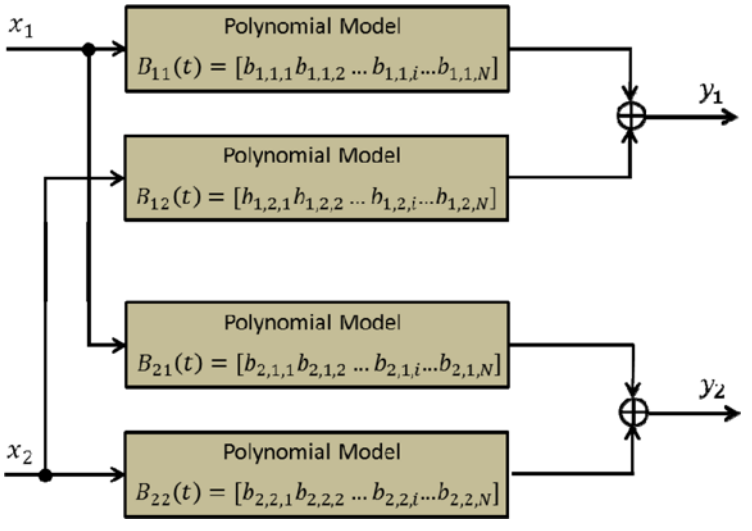

Fig. 6.17 Modeling of a 2×2 MIMO transmitter with nonlinear crosstalk

In addition to crosstalk, the I/Q imbalance of the modulator affects the performance of the MIMO transmitter. The modeling of the I/Q imbalance of the modulator is based on the modeling of the cross coupling channels between the I and Q components of the modulator signal input. The cross coupling terms can be presented in the model by utilizing the conjugate of the input signal [18]. I/Q imperfections are generally gain and phase imbalance and DC offset. The signal at the output of a SISO transmitter suffering from such impairments can be expressed as:

$$\begin{aligned} y(n) &= \sum_{j=0}^{M}\sum_{i=1}^{N} b_{i,j}\cdot x(n-j)\cdot\left|x(n-j)\right|^{i-1} \\ &+\sum_{j=0}^{M}\sum_{i=1}^{N} b'_{i,j}\cdot x^{*}(n-j)\cdot\left|x(n-j)\right|^{i-1} + b_{dc} \end{aligned} \tag{6.14}$$

where $x(n)$, $x^{*}(n)$ and $y(n)$ are the input, input conjugate and output complex signals envelopes, respectively; and, b_{dc} is a DC term used to estimate the DC offset of the modulator.

Figure 6.18 demonstrates the modeling of the modulator's I/Q imbalance for a SISO transmitter for the memoryless case.

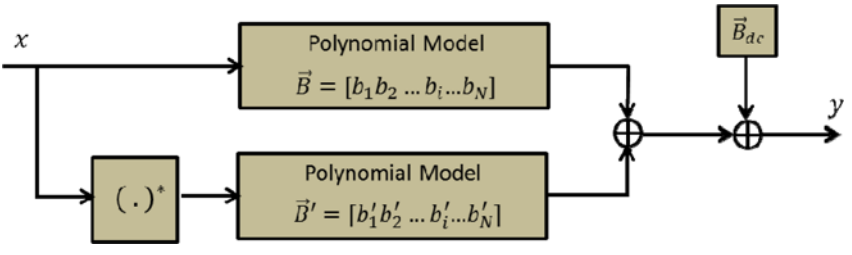

Fig. 6.18 Modeling of modulator I/Q imbalance for a SISO transmitter

Based on the prior models, a dual-input dual-output MIMO transmitter that suffers from PA nonlinearity, modulator I/Q imbalance and coupling effects can be counted as a nonlinear system with four inputs (x_1, x_2, x_1^{*}, x_2^{*}) and two outputs (y_1, y_2). The outputs can be related to the inputs as:

$$\begin{bmatrix} y_1 & y_2 \end{bmatrix}^T = \mathbf{W}\begin{bmatrix} x_1 & x_2 & x_1^{*} & x_2^{*} \end{bmatrix}^T \tag{6.15}$$

where $\mathbf{W}$ is a nonlinear matrix function that characterizes the behavior of the transmitter. The signal at the output of the MIMO transmitter suffering from PAs nonlinearity, nonlinear crosstalk, modulator I/Q imbalance and DC offset can be expressed as:

$$y_k(n) = \sum_{j=0}^{M}\sum_{i=1}^{N} b_{k,1,i,j} \cdot x_1(n-j) \cdot \left|x_1(n-j)\right|^{i-1} +$$
$$\sum_{j=0}^{M}\sum_{i=1}^{N} b'_{k,1,i,j} \cdot x_1^*(n-j) \cdot \left|x_1(n-j)\right|^{i-1} +$$
$$\sum_{j=0}^{M}\sum_{i=1}^{N} b_{k,2,i,j} \cdot x_2(n-j) \cdot \left|x_2(n-j)\right|^{i-1} +$$
$$\sum_{j=0}^{M}\sum_{i=1}^{N} b'_{k,2,i,j} \cdot x_2^*(n-j) \cdot \left|x_2(n-j)\right|^{i-1} + b_{dc}$$

Digital baseband preprocessing techniques can be used to compensate for all the effects previously mentioned. Hence, identification needs to be performed to extract the coefficients of the inverse model. The inverse model is used to generate the MIMO transmitter input when fed with the MIMO transmitter output.

References

[1] Duman, T.M., Ghrayeb, A.: Coding for MIMO Communication Systems. Wiley (2008)

[2] Mohammadi, A., Ghannouchi, F.M.: Single RF Front-End MIMO Transceivers. IEEE Communications Magazine (December 2011)

[3] Bassam, S.A., Helaoui, M., Ghannouchi, F.M.: Crossover Digital Predis-torter for the Compensation of Crosstalk and Nonlinearity in MIMO Transmitters. IEEE Transactions on Microwave Theory and Techniques 57(5), 1119–1128 (2009)

[4] Lari, M., Bassam, S.A., Mohammadi, A., Ghannouchi, F.M.: Time-Multiplexed Single Front-End Multiple-Input Multiple-Output Receivers with Preserved Diversity Gain. IET Communications 5(6), 789–796 (2011)

[5] Molisch, A., Win, M., Winters, J.: Reduced-Complexity Trans-mit/Receive-Diversity Systems. IEEE Transactions on Signal Processing 51(11), 2729–2738 (2003)

[6] Tzeng, F., Jahanian, A., Pi, D., Heydari, P.: A CMOS code-modulated path-sharing multi-antenna receiver front-end. IEEE Journal of Solid-State Circuits 44(5), 1321–1335 (2009)

[7] Vankka, J.: Digital Synthesizers and Transmitters for Software Radio. Springer, Heidelberg (2005)

[8] Bassam, S.A., Boumaiza, S., Ghannouchi, F.M.: Block-Wise Estimation of and Compensation for I/Q Imbalance in Direct-Conversion Transmitters. IEEE Transactions on Signal Processing 57(12), 4970–4973 (2009)

[9] Wiser, R.: Tunable Bandpass RF Filters for CMOS Wireless Transmitters. ProQuest (2008)

[10] Gesbert, D., Shafi, M., Shiu, D.-S., Smith, P.J., Naguib, A.: From Theory to Practice: An Overview of MIMO Space-Time Coded Wireless Systems. IEEE Journal on Selected Areas in Communications 21(3) (April 2003)

[11] Molisch, A.F., Win, M.Z., Winters, J.H.: Reduced-Complexity Transmit/Receive Diversity Systems. In: Proc. IEEE Vehicular Technology Conference, pp. 1996–2000 (May 2001)

[12] Jahanian, A., Tzeng, F., Heydari, P.: Code-Modulated Path-Sharing Multi-Antenna Receivers: Theory and Analysis. IEEE Transactions on Wireless Communications 8(5), 2193–2201 (2009)

[13] Bassam, S.A., Helaoui, M., Boumaiza, S., Ghannouchi, F.M.: Experimental Study of the Effects of RF Front-End Imperfection on the MIMO Transmitter Performance. In: Proc. IEEE MTT-S International Symposium Digest, pp. 1187–1190 (June 2008)

[14] Palaskas, Y., Ravi, A., Pellerano, S., Carlton, B.R., Elmala, M.A., Bishop, R., Banerjee, G., Nicholls, R.B., Ling, S.K., Dinur, N., Taylor, S.S., Soumyanath, K.: A 5-GHz 108-Mb/s 2 ×2 MIMO Transceiver RFIC with Fully In-tegrated 20.5-dBm P_{1dB} Power Amplifiers in 90-nm CMOS. IEEE Journal of Solid-State Circuits 41(12), 2746–2756 (2006)

[15] Tse, D., Viswanath, P.: Fundamentals of Wireless Communication. Cambridge University Press, Cambridge (2005)

[16] Medvedev, I., Bjerke, B.A., Walton, R., Ketchum, J., Wallace, M., Howard, S.: A Comparison of MIMO Receiver Structures for 802.11n WLAN—Performance and Complexity. In: The 17th Annual IEEE International Symposium on Personal, Indoor, and Mobile Radio Communications, Helsinki, Finland (September 2006)

[17] Ghannouchi, F.M., Hammi, O.: Behavioural Modeling and Predistortion. IEEE Microwave Magazine 10(7), 52–64 (2009)

[18] Anttila, L., Handel, P., Valkama, M.: Joint Mitigation of Power Amplifier and I/Q Modulator Impairments in Broadband Direct-Conversion Transmitters. IEEE Transactions on Microwave Theory and Techniques 58(4) (April 2010)